Article **Journal Innovative Design**
June, 2022 Vol.6 No.15 10-18

Neural Sliding mode control of a regenerative braking system for electric vehicles

Control Neuronal por modos deslizantes para el frenado regenerativo de vehículos eléctricos

RUZ-CANUL, Mario Antonio†*, DJILALI, Larbi, RUZ-HERNANDEZ, José Antonio and SANCHEZ-CAMPEROS, Edgar Nelson

Universidad Autónoma del Carmen, Facultad de Ingeniería

ID 1st Author: *Mario Antonio, Ruz-Canul* / **ORC-ID:** 0000-0003-0872-062X, **CVU CONACYT ID**: 1085717

ID 1st Coauthor: *Larbi, Djilali* / **ORC-ID:** 0000-0002-3594-5747, **CVU CONACYT ID:** 696839

ID 2nd Coauthor: *José Antonio, Ruz-Hernández* / **ORC ID**: 0000-0001-8332-4980, **CVU CONACYT ID**: 216374

ID 3rd Coauthor: *Edgar Nelson, Sánchez-Camperos* /**ORC ID:** 0000-0002-8695-7879, **CVU CONACYT ID**: 597

DOI: 10.35429/JID.2022.15.6.10.18 Received July 23, 2022; Accepted October 30, 2022

Abstract

This paper summarizes the work done on the development of a Neural Sliding Mode Controller (NSMC) for a regenerative braking system used in an electric vehicle (EV), which is composed of a Main Energy System (MES) and an Auxiliary Energy System (AES). This last one contains a buck-boost converter and a super-capacitor. The AES aims to recover the energy generated during braking that the MES cannot retrieve and use later during acceleration. A neural identifier trained with the Extended Kalman Filter (EKF) has been used to estimate the buck-boost converter real dynamics and to build up the NSMC, which is implemented to regulate the voltage and current dynamics in the AES. Simulation results**,** illustrate the effectiveness of the proposed control scheme to track time-varying references of the AES voltage and current dynamics measured at the buck-boost converter and ensure the charging and discharging operation modes of the super-capacitor. In addition, the proposed control scheme enhances the EV storage system efficiency and performance, when the regenerative braking system is employed.

Regenerative Braking, Sliding Mode Controller, Electrical Vehicle.

Resumen

Este articulo recopila el trabajo realizado en el desarrollo de un Control por Modos Deslizantes Neuronal (NSMC) para el frenado regenerativo utilizado en un vehículo eléctrico, el cual está conformado por un Sistema Principal de Energía (MES) y un Sistema Auxiliar de Energía (AES). Este último contiene un convertidor elevador-reductor y un super capacitor. El objetivo del AES es recuperar la energía generada durante el frenado que el MES no puede recuperar y utilizarla después durante la aceleración. Un identificador neuronal entrenado con el Filtro de Kalman Extendido (EKF) ha sido utilizado para estimar las dinámicas reales del convertidor elevador-reductor y para diseñar el NSMC, el cual es implementado para regular el voltaje y la corriente en el AES. Los resultados de la simulación ilustran la efectividad del esquema de control propuesto para el seguimiento de referencias variables en el tiempo del voltaje y corriente del AES medidas en el convertidor elevador-reductor y el mejoramiento de los modos de operación de carga y descarga del super capacitor. Además, el esquema de control propuesto mejora la eficiencia y el rendimiento del sistema de almacenamiento del EV, cuando el sistema de frenado regenerativo es empleado.

Frenado regenerativo, Control por Modos Deslizantes, Vehículo Eléctrico

Citation: RUZ-CANUL, Mario Antonio, DJILALI, Larbi, RUZ-HERNANDEZ, José Antonio and SANCHEZ-CAMPEROS, Edgar Nelson. Neural Sliding mode control of a regenerative braking system for electric vehicles. Journal Innovative Design. 2022, 6-15: 10-18

*Correspondence to the Author (e-mail: 120664@mail.unacar.mx)
† Researcher contributing as first author.

© ECORFAN- Taiwan

I. Introduction

Nowadays, Electric Vehicles (EVs) present an important alternative solution to conventional vehicles, regarding gasoline prices, gas emissions, and climatic changes among other factors [1]. In EVs, electric motors can be controlled to be operated as generators to convert the kinetic or potential energy of vehicle mass into an electric one, which can be stored and utilized to improve the driving performance and extend the life of the storage system [2].

Different proposals have been developed to enhance the efficiency of EVs. One of the implemented solutions is called hybrid vehicles, which combine an internal combustion engine and an electric car motor improving the emission of exhaust gases over internal combustion vehicles [3]. Another type of hybrid vehicle has emerged, named the plug-in hybrid electric vehicle, which allows drivers to charge the battery bank using an external EV charger [4]. By using these technologies, various benefits can be achieved; however, the hybrid nature of these EVs required more complex hybrid controllers and communication systems to ensure the switching between both installed supply systems [5]. These challenges can be reduced by using fully-EVs technology using the combination of a Main Energy System (MES) and an Auxiliary Energy System (AES) based battery bank, super-capacitor, and power electronic devices, which provide an extended driving range, high power quality, regenerative braking capability, and better system efficiency [6].

Recently, the regenerative braking capability in EVs is one of the most important characteristics of EVs, which helps to recover energy during braking and enhances the storage system efficiency [7]. Different control methodologies and regenerative braking architectures have been investigated and implemented in the last years. In [8], a design of the regenerative braking for EV with help of an ultra-capacitor pack and battery is developed where the objective is to save the wasted energy during braking. Results illustrate that the additional super-capacitor pack improves the efficiency of the regenerative braking in comparison with the standalone battery system.

The same design is implemented in [9] where a Proportional-Integral (PI) controller is used to regulate the buck-boost converter output voltage related to the super-capacitor pack.

In [10] a fuzzy logic sliding mode controller is implemented using the exponential reaching law and parameter optimizing for an anti-lock braking system to keep the optimal slip value on the braking system of the EV. In [11] an intelligent sliding mode controller is employed to track the desired slip during a braking scenario; the obtained results illustrate a considerable energy recuperation without overcharging in the battery bank compared with the fuzzy sliding mode control developed in [10] and the Fuzzy one in [12].

Unfortunately, all controllers previously described required prior knowledge of system parameters, which are not always reachable in real cases. In addition, those control methodologies are not robust to disturbances, which affect system stability and system efficiency [13].

Regarding technology advances, complex unknown dynamics, and highly coupled behaviors are introduced, which force the control engineers to use appropriate mathematical tools to deal with control problems. Recently, Neural Networks (NNs) have been widely implemented in the approximation of unknown dynamics, then based on the obtained model, conventional controllers are developed. Different control problems are solved using neural control such as in multiagent stabilization systems [14], microgrids [15], biomedical applications [16], among others.

However, the EVs and regenerative braking system are less investigated using this neural control strategy [17]. This paper presents Neural Sliding Mode Controller (NSMC) for a regenerative braking system. The proposed controller is used to control the current and voltage of the buck-boost converter related to AES with the objective to recover the waste energy during braking and enhance the MES efficiency.

ISSN-2523-6830
ECORFAN® All rights reserved

The main contribution of the present paper is: 1) an online identification based Recurrent High Order Neural Network (RHONN) trained by the Extended Kalman Filter (EKF) is a build-up to approximate the DC buck-boost behaviors. 2) Based on the obtained neural model, the sliding mode is synthesized and implemented to track the buck-boost current and voltage desired dynamics. 3) since the proposed controller is based on the neural identifier, robustness to parameter variations and disturbances is ensured; in addition, chattering is significantly reduced on the tracked dynamics. 4) by the implementation of the proposed controller for the AES, the storage energy in MES is improved, moreover, energy lost is largely reduced in comparison with standalone MES. The paper is organized as follows: In section 2, the regenerative braking problem is described.

In section 3, mathematical preliminaries are introduced. In section 4, the system modeling, identification and control for the buck-boost converter are developed. In section 5, simulation results are presented.

Desarrollo de Secciones y Apartados del Artículo con numeración subsecuente

II. Regenerative Braking System

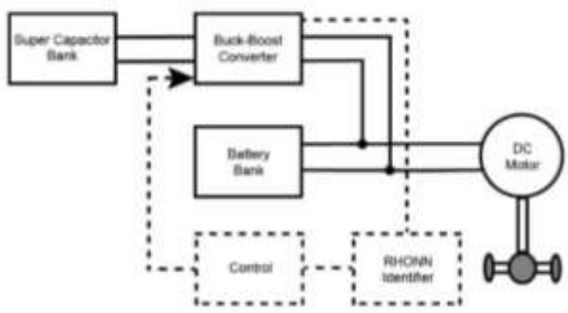

Figure 1 Regenerative Braking System

A regenerative braking system as depicted in Fig. 1 allows the recovery of kinetic energy produced during braking and its utilization to improve the energy storage efficiency and extend the operating distance of the EV [2]. This system is composed of a super-capacitor and buck-boost converter, which are part of the AES. In addition, a battery bank is used to administrate the energy to the electrical motor conforming to the MES.

The super-capacitor and the buck-boost converter are connected as illustrated in Fig. 2, with the objective of increasing or decreasing the output voltage depending on the following operation modes.

Buck operation

In this mode, the output voltage is decreased from the input voltage. To achieve such, T1 is OFF and T2 is activated, consequently, the energy is transferred from the capacitor (Vc) to the super-capacitor voltage (Vsc). When T2 is turned on, current flows from capacitor C, generating the Ic current to the super-capacitor. As the result, a fraction of this energy is charged into the inductance L. On the other hand, when T2 is turned off the current charged in L is discharged into Vc through the diode D1, driving the current in the direction of capacitor C [9].

Boost operation

On the other hand, in this mode, the output voltage is increased. To do such, T2 is deactivated and T1 is activated to transfer energy from the super-capacitors Vsc to the battery bank V c. When T1 is ON, the energy is acquired from the capacitor and stored in the inductance L.
Reversely, when T1 is OFF, the energy stored in the inductance is transferred into the capacitor through the diode D2 and keep it in the battery bank.

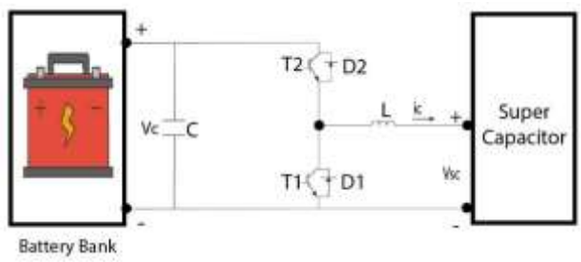

Figure 2 Buck-Boost Converter

During the braking operation, the brake manages the electricity generated by the motor into the batteries or capacitors. The DC-DC converter operates in boost function during acceleration while it operates into buck function in deceleration, which will make it easier in charging up the super-capacitor.

ECORFAN® All rights reserved

III. Mathematical Preliminaries

A. Discrete-Time Recurrent High Order Neural Networks

Recently, recurrent neural networks have been used in many applications and give excellent results in nonlinear dynamics approximations [13]. However, RHONN has demonstrated that is a good choice in nonlinear systems identification, which consists of adjusting the parameters of an appropriately selected model according to an adaptive law. Using a series-parallel configuration, the estimated state variable of a nonlinear system using the RHONN identifier is given by [18]

$$\chi_{i,k+1} = \omega_i^T \phi_i(x_k, u_k, k) \quad (1)$$

where $\chi_{i,k+1}$ is the state of the i^{th} neuron which identifies the i^{th}component of x_k, $x_k = [x_{1,k}, \dots, x_{n,k}]$is the state vector, $\omega_{i,k} \in \mathrm{R}^{L_i}$ are the adjustable synaptic weights of NNs, $u \in \mathrm{R}^m$ is the input vector, and $\phi_i(x_k, u_k, k) \in \mathrm{R}^{L_i}$is defined as [13].

$$\phi_i(x_k, u_k, k) = \begin{bmatrix} \phi_{i_1} \\ \phi_{i_k} \\ \vdots \\ \phi_{i_{L_i,k}} \end{bmatrix} = \begin{bmatrix} \prod_{j \in I_1} \zeta_{ij}^{d_{ij(1)}} \\ \prod_{j \in I_2} \zeta_{ij}^{d_{ij(2)}} \\ \vdots \\ \prod_{j \in I_{L_i}} \zeta_{ij}^{d_{ij(L_i)}} \end{bmatrix} \quad (2)$$

where $d_{ij,k}$are non-negative integers, L_i is the connection number, $I_1, I_2, \dots I_{L_i}$ is a non-ordered subset collection of $1,2 \dots, n+m$, n is the state dimension, m is the inputs dimension, and ζ_i is defined as [13].

$$\zeta_i = \begin{bmatrix} \zeta_{i_1} \\ \vdots \\ \zeta_{i_n} \\ \vdots \\ \zeta_{i_{n+m}} \end{bmatrix} = \begin{bmatrix} S(x_1) \\ \vdots \\ S_{x_n} \\ u_{1,k} \\ \vdots \\ u_{m,k} \end{bmatrix} \quad (3)$$

Where$u = [u_{1,k}, u_{2,k}, \dots, u_{m,k}^T]$ is the input vector to the network. The function $S(.)$ is a hyperbolic tangent function defined as

$$S(x_k) = \alpha_i \tanh(\beta_i x_k) \quad (4)$$

where x_k is the state variable; α and β are positive constants. To approximate a nonlinear model, the discrete-time RHONN in (1) is modified as [19].

$$\chi_{i,k+1} = \omega_i^T \phi_i(x_k) + \overline{\omega}_i^T \varphi_i(x_k, u_k) \quad (5)$$

where $\omega_{i,k}$ represents the adjustable weights, and $\overline{\omega}_{i,k}$ is fixed weights, φ_i is a linear function of the state vector or vector input u_k depending to the system structure or external inputs to the RHONN model. Fig. 3 illustrates an i^{th} RHONN identifier scheme.

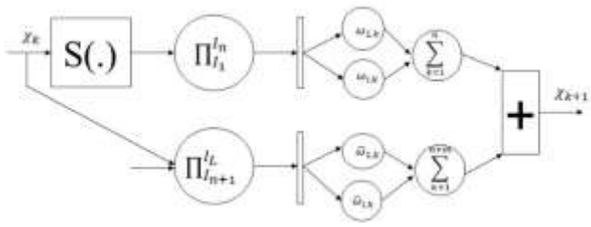

Figure 3 RHONN Scheme

B. Discrete-Time Sliding Mode Control

In the last decades, the sliding mode controller receives much attention due to its robustness to some class of perturbation. Consider the following nonlinear system [20]

$$\dot{x} = f(x, u, t) \quad (6)$$

with the bounded function $f(x)$, $|f(x)| < f_o =$ constant and the control law, as a relay function, which is used to track the error $e = r(t) - x$, $r(t)$ to zero where is the reference input, and u is defined as

$$u = \begin{cases} u_0 & if \quad s(x) \geq 0 \\ -u_0 & if \; s(x) < 0 \end{cases} \quad (7)$$

where $s(x)$ and u_0 are define as the sliding surface and the upper control bound, respectively.

Fig. 4 illustrates the behavior of the continuous-time system with scalar sliding mode control, where the state $x(t)$ initiates from an initial point $x(t=0)$, the trajectory reaches the sliding surface $S(x) = 0$ within finite time t_{sm} and remains on the surface subsequently.

ECORFAN® All rights reserved

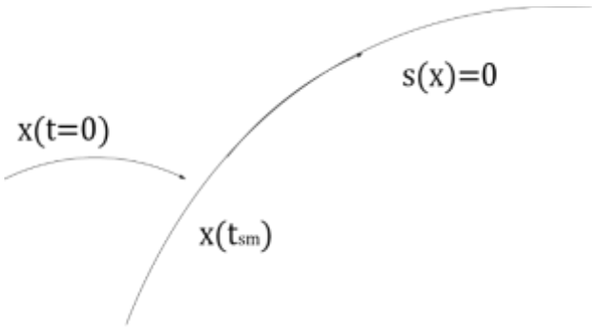

Figure 4 Motion trajectory of continuous system with scalar sliding mode control

When for each sampling point the function is derived $t_j = k\Delta t,\ k = 1,2\ldots$, the representation of the continuous time system in discrete time in (6) is

$$x_{k+1} = F(x_k) \tag{8}$$

with the condition that starting from t_{sm}, the trajectory belongs to the sliding manifold with $s(x(t))$, or for a $k_m \geq t_{sm}/\Delta t$ [20].

$$s(x_k) = 0 \qquad \forall k \geq k_{sm} \tag{9}$$

This motion can be defined as discrete time sliding mode. Consequently, from (6) and in scenario where for any constant control u and any initial condition $x(0)$, its solution can be written in closed form as [21].

$$x(t) = F(x(0), u) \tag{10}$$

with u_k should be selected at each sampling point k such that this constant control signal will achieve $s(x_{k+1})$. The discrete-time system is defined as [21].

$$x_{k+1} = F(x_k, u_k) \tag{11}$$

$$u_k = u(x_k) \tag{12}$$

The sliding manifold is attained at each sampling point i.e., $s(k_{k+1}),\quad \forall k = 0,1,\ldots$ is fulfilled.

This is true because $F(x(0), u)$ tends to $x(0)$ as $\Delta t \to 0$, the function $u(x(0), \Delta t)$ may exceed the available control resources u_0 Using the discrete time sliding mode, the sliding manifold is defined as

$$s(x_k) = x_k - x_{ref,k} \tag{13}$$

Evaluating the sliding manifold at $(k+1)$, we obtain

$$s_{k+1} = F(x_k, u_k) - x_{ref,k+1} \tag{14}$$

Then, the equivalent control $u_{eq}(x_k, k)$ is calculated as [20]

$$u_{eq}(x_k, k) = -\left[F(x_k, k) - x_{ref,k+1}\right] \tag{15}$$

It is appropriate to add a stabilizing term $u_n(x_k, k)$, to reach the sliding manifold asymptotically [21]

$$u_n(x_k, k) = -(ks_k) \tag{16}$$

where k is Schur matrix.

Considering the boundedness of the control signal $\| u_c(x_k, k) \| < u_0\ ,\ u_0 > 0$, the following control law is selected [20]

$$u(x_k, k) = \begin{cases} u_c(x_k, k) & if\ \ ||u_c(x_k, k)|| < u_0 \\ u_0 \dfrac{u_{eq}(x_k, k)}{\left||u_{eq}(x_k, k)|\right|} & if\ \ ||u_c(x_k, k)|| \geq u_0 \end{cases} \tag{17}$$

Where $||.||$stands for the Euclidean norm and $u_c(x_k, k) = u_{eq}(x_k, k) + u_n(x_k, k)$.

IV. Buck-Boost Neural Control Analysis

A. System Modeling

The used DC-DC converter in this application is composed of a boost and buck converters. The first one is used under charge conditions while the second one is used under discharge conditions. The boost converter model is defined as [22].

$$x_{1,k} = \left(1 - \frac{ts}{RC}\right) x_{1,k} - \frac{ts}{c} x_{2,k} \tag{18}$$

$$x_{2,k} = x_{2,k} + \frac{ts}{L} U_{btt} u_c \tag{19}$$

The buck converter model is given by [22]

$$x_{1,k} = \left(1 - \frac{ts}{RC}\right) x_{1,k} + \frac{ts}{c} x_{2,k} \tag{20}$$

$$x_{2,k} = x_{2,k} + \frac{ts}{L} U_{btt} u_c \tag{21}$$

ISSN-2523-6830
ECORFAN® All rights reserved

where $x_{1,k}$ is the Buck-Boost converter output voltage, $x_{2,k}$ is the Buck-Boost converter output current both with the inductance L(H), resistance load R (Ω), capacitor (F) C, and t_s sampling time.

B. Neural Controller Design

To control the current flow and ensure the charging and discharging operation modes, an RHONN has been used to approximate the buck-boost converter behaviors and then the sliding mode controller is synthesized. Knowing the adaptive nature of the RHONN, and the similitude between the buck and boost converter models a single identifier is proposed for both cases as

$$\widehat{x_{1,k}} = \omega_{1,1}(k)S(x_1) + \omega_{1,2}(k)S(x_2) + w_{1,3}S(x_1)S(x_2) + \varpi_1 x_2 \quad (22)$$

$$\widehat{x_{2,k}} = \omega_{2,1}(k)S(x_2) + \omega_{2,2}(k)S(x_1) + w_{2,3}S(x_1)S(x_2) \quad (23)$$

Equations (22) and (23) can be rewritten as follows

$$\widehat{x_k} = \hat{F}(x_k) + \hat{B}u(x_k, k) \quad (24)$$

$$\widehat{y_k} = x_{2,k}k \quad (25)$$

where $\left[\widehat{x_{1,k}}, \widehat{x_{2,k}}\right]^T$ are the estimated dynamics of $\left[x_{1,k}, x_{2,k}\right]^T$, u_k is the input signal, $\widehat{y_k}$ is the output to be tracked, and $\hat{B}$ is the control matrix defined as $\hat{B} = diag[0, \varpi_2]$. Since the proposed neural model is formulated in the triangular form, the control of the last dynamics is only needed [20]. So, by using the same steps as in (11)-(17) the sliding surface at $k+1$ is obtained as

$$s_{k+1} = \omega_{2,1}(k)S(x_2) + \omega_{2,2}(k)S(x_1) + w_{2,3}S(x_1)S(x_2)\varpi_2 u(x_k, k) - x_{ref,k+1} \quad (26)$$

Then, the equivalent control is calculated as follows

$$u_{eq}(x_k, k) = -\frac{1}{\varpi_2}\left[\omega_{2,1}(k)S(x_2) + \omega_{2,2}(k)S(x_1) + w_{2,3}S(x_1)S(x_2) - x_{ref,k+1}\right] \quad (27)$$

And the NSMC is implemented as follows.

$$u(x_k, k) = \begin{cases} u_c(x_k, k) & if \ ||u_c(x_k, k)|| < u_0 \\ u_0 \frac{u_{eq}(x_k, k)}{||u_{eq}(x_k, k)||} & if \ ||u_c(x_k, k)|| \geq u_0 \end{cases} \quad (28)$$

With $u_c(x_k, k) = u_{eq}(x_k, k) + u_n(x_k, k)$, $u_n(x_k, k) = -(ks_k)$, where k is Schur matrix, and u_0 is the control upper bound.

V. Simulation results

The proposed control scheme as well the respective MES and AES are implemented and evaluated using the SimPower System toolbox of MATLAB. The parameters of the AES and MES are listed in Tab. 1

Description	Unit
Converter Resistance R.	50 Ω
Converter Inductance L	1.5 $e^{-3}H$
Converter Capacitance C	100 e^{-3} F
Super-capacitor voltage V_{sc}	350 V
Battery Bank Voltage V_c	450 V
Initial SOC	80%
Sampling time (t_s)	$1e^{-5}s$

Table 1 Parameters of the AES and MES

A. Neural Identification

The implemented RHONN identification allows to achieve adequate estimation of system states, which are in this case, the voltage x_1, k and current x_2, k during different operation modes. Fig.5 illustrates the neural identification of the voltage $(x_1, k)$and their respective neural weights evolution.

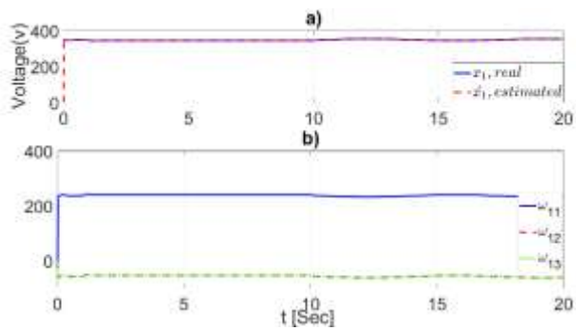

Figure 5 a) Voltage identification (x_1, k) b) NN_s weights

Fig. 6 presents the neural identification of the current (x_2, k) and their respective neural weights dynamics.

ECORFAN® All rights reserved

From the obtained results, it is clear to observe that the proposed RHONN identifiers successfully approximate the voltage and current dynamics of the AES even a varying-time trajectories are applied. In addition, all neural weights are bounded.

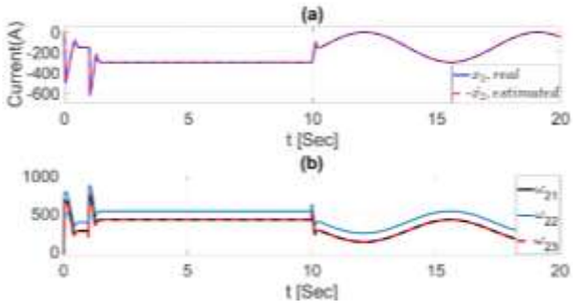

Figure 6. a) Current identification (x_2, k) b) NN_s weights

B. Trajectory Tracking

In this test, the objective is to demonstrate the trajectories tracking of the AES voltage and current. To do such, a varying-time voltage reference x_1, r is used where it is initiated in $350\ V$ and then decrease to $345\ V$ after $10\ s$ and then, this reference is changed to a sinusoidal function. Fig 7 presents the obtained results for the voltage (x_1, k) at the output of the Buck-boost converter used in the AES system, which is controller using NSMC.

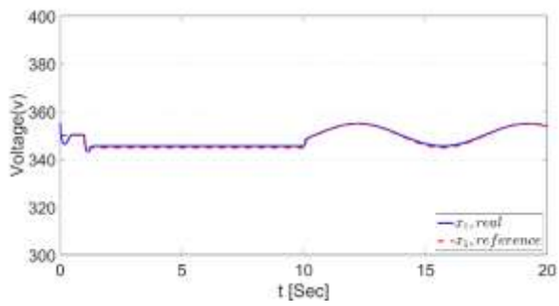

Figure 7 Voltage Trajectory Tracking

Fig 8 demonstrates the behavior of the current (x_2, k) as measured at inductor of the Buck-boost converter.

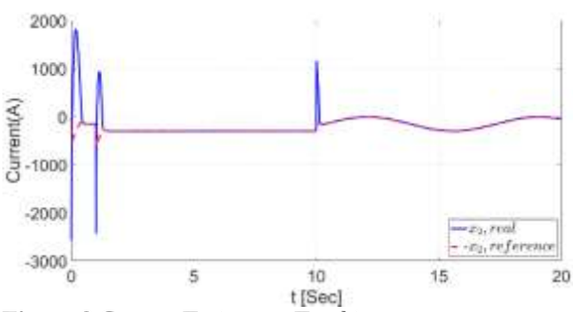

Figure 8 Current Trajectory Tracking

Fig. 9 displays the charging and discharging modes of the AES. In the charging operating mode, $t = 0\ s$ to $t = 10\ s$, the boost mode is selected while the buck mode is used during the discharging mode $t = 10\ s$ to $t = 20\ s$.

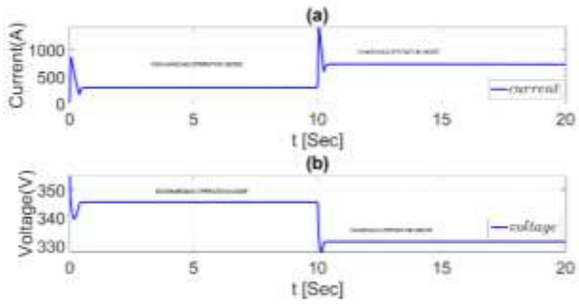

Figure 9 AES charging and discharging

From the obtained results, we can see that the proposed control scheme (NSMC) ensures adequate trajectories tracking of the AES voltage and current even a time-varying references are applied. In addition, the proposed controller assures the charge and discharge operation modes of the AES.

Fig. 10 illustrates a comparison between the MES discharging behavior with and without AES. Form the obtained results, the MES performance is improved by using the AES since the MES discharging behavior without AES is fast than when this last is activated.

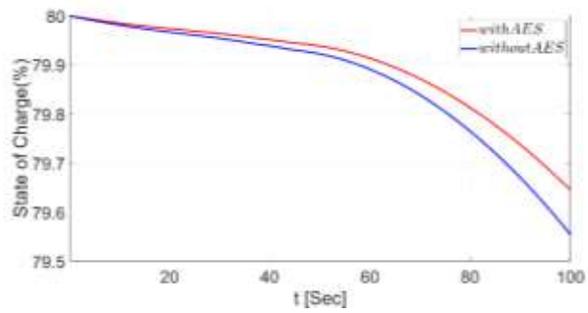

Figure 10 Comparison of variables with and without the regenerative braking

VI. Conclusion

This paper presents NSMC of a regenerative braking system used in the EVs. The proposed control scheme is used to control the AES composed of a buck-boost converter and super-capacitor with the objective to recover the energy during breaking and participating in power supply of the MES.

ECORFAN® All rights reserved

The RHONN identifier trained by an EKF is build-up to approximate the AES behavior under different operation modes; then, the Sliding mode controller is synthesized. The proposed control scheme is tested for trajectory tracking of time-varying references and in the presence of AES different operation modes. The obtained results illustrate the effectiveness of the proposed control scheme where the trajectories tracking of AES voltage and current are achieved and the charging and discharging mode is ensured. In addition, the MES behavior is enhanced by using the AES, which helps to improve the discharging time of the MES and extend the operation time of the EV.

As a future work, the proposed control scheme and other ones will be implemented in real-time and tested in the presence of parameter variation and disturbances.

Finally, the used controller in this paper presents a simple control algorithm, which can be used in the industrial EV applications.

Acknowledgments

This work has been funded by Consejo Nacional de Ciencia y Tecnología (CONACYT) [1085717] and Universidad Autónoma del Carmen (UNACAR) [120664].

References

[1] Pavlović, T., Mirjanić, D., Mitić, I. R., & Stanković, A. M. (2019, June). The Impact of Electric Cars Use on the Environment. In *International Conference "New Technologies, Development and Applications"* (pp. 541-548). Springer, Cham. https://doi.org/10.1007/978-3-030-18072-0_62

[2] Yoong, M. K., Gan, Y. H., Gan, G. D., Leong, C. K., Phuan, Z. Y., Cheah, B. K., & Chew, K. W. (2010, November). Studies of regenerative braking in electric vehicle. In *2010 IEEE Conference on Sustainable Utilization and Development in Engineering and Technology* (pp. 40-45). IEEE. https://doi.org/10.1109/STUDENT.2010.5686984

[3] Tie, S. F., & Tan, C. W. (2013). A review of energy sources and energy management system in electric vehicles. *Renewable and sustainable energy reviews*, *20*, 82-102. https://doi.org/10.1016/j.rser.2012.11.077

[4] García-Villalobos, J., Zamora, I., San Martín, J. I., Asensio, F. J., & Aperribay, V. (2014). Plug-in electric vehicles in electric distribution networks: A review of smart charging approaches. *Renewable and Sustainable Energy Reviews*, *38*, 717-731. https://doi.org/10.1016/j.rser.2014.07.040

[5] Hannan, M. A., Azidin, F. A., & Mohamed, A. (2014). Hybrid electric vehicles and their challenges: A review. *Renewable and Sustainable Energy Reviews*, *29*, 135-150. https://doi.org/10.1016/j.rser.2013.08.097

[6] Ortúzar, M., Moreno, J., & Dixon, J. (2007). Ultracapacitor-based auxiliary energy system for an electric vehicle: Implementation and evaluation. *IEEE Transactions on industrial electronics*, *54*(4), 2147-2156. https://doi.org/10.1109/TIE.2007.894713

[7] Zhang, L., & Cai, X. (2018). Control strategy of regenerative braking system in electric vehicles. *Energy Procedia*, *152*, 496-501. https://doi.org/10.1016/j.egypro.2018.09.200

[8] Indragandhi, V., Selvamathi, R., Gunapriya, D., Balagurunathan, B., Suresh, G., & Chitra, A. (2021, November). An Efficient Regenerative Braking System Based on Battery-Ultracapacitor for Electric Vehicles. In *2021 Innovations in Power and Advanced Computing Technologies (i-PACT)* (pp. 1-5). IEEE. https://doi.org/10.1109/i-PACT52855.2021.9696557

[9] Quintero-Manriquez, E., Sanchez, E. N., Antonio-Toledo, M. E., & Munoz, F. (2021). Neural control of an induction motor with regenerative braking as electric vehicle architecture. *Engineering Applications of Artificial Intelligence*, *104*, 104275. https://doi.org/10.1016/j.engappai.2021.104275

ECORFAN® All rights reserved

[10] J. Guo, J. Xiaoping, and L. Guangyu, "Performance evaluation of an anti-lock braking system for electric vehicles with a fuzzy sliding mode controller," Energies, vol. 7, pp. 6459–6476, Aug. 2014. https://doi.org/10.3390/en7106459

[11] Rajendran, S., Spurgeon, S., Tsampardoukas, G., & Hampson, R. (2018). Intelligent sliding mode scheme for regenerative braking control. *IFAC-PapersOnLine*, *51*(25), 334-339. https://doi.org/10.1016/j.ifacol.2018.11.129

[12] Li, X., Xu, L., Hua, J., Li, J., & Ouyang, M. (2008, October). Regenerative braking control strategy for fuel cell hybrid vehicles using fuzzy logic. In *2008 International Conference on Electrical Machines and Systems* (pp. 2712-2716). IEEE.

[13] Sanchez, E. N., Alanís, A. Y., & Loukianov, A. G. (2008). *Discrete-time high order neural control*. Warsaw: Springer. https://doi.org/10.1007/978-3-540-78289-6

[14] Lopez-Franco, M., Sanchez, E. N., Alanis, A. Y., Lopez-Franco, C., & Arana-Daniel, N. (2015). Decentralized control for stabilization of nonlinear multi-agent systems using neural inverse optimal control. *Neurocomputing*, *168*, 81-91. https://doi.org/10.1016/j.neucom.2015.06.012

[15] Djilali, L., Vega, C. J., Sanchez, E. N., & Ruz-Hernandez, J. A. (2021). Distributed Cooperative Neural Inverse Optimal Control of Microgrids for Island and Grid-Connected Operations. *IEEE Transactions on Smart Grid*, *13*(2), 928-940. https://doi.org/10.1109/TSG.2021.3132640

[16] Rios, Y. Y., Garcia-Rodriguez, J. A., Sanchez, E. N., Alanis, A. Y., & Ruiz-Velázquez, E. (2018, November). Rapid Prototyping of Neuro-Fuzzy Inverse Optimal Control as Applied to T1DM Patients. In *2018 IEEE Latin American Conference on Computational Intelligence (LA-CCI)* (pp. 1-5). IEEE. https://doi.org/10.1109/LA-CCI.2018.8625241

[17] Cao, J., Cao, B., Xu, P., & Bai, Z. (2008, July). Regenerative-braking sliding mode control of electric vehicle based on neural network identification. In *2008 IEEE/ASME International Conference on Advanced Intelligent Mechatronics* (pp. 1219-1224). IEEE. https://doi.org/10.1109/AIM.2008.4601836

[18] Alanis, A. Y., Sanchez, E. N., & Loukianov, A. G. (2007). Discrete-time adaptive backstepping nonlinear control via high-order neural networks. *IEEE Transactions on Neural Networks*, *18*(4), 1185-1195. https://doi.org/10.1109/TNN.2007.899170

[19] Rovithakis, G. A., & Christodoulou, M. A. (2012). *Adaptive control with recurrent high-order neural networks: theory and industrial applications*. Springer Science & Business Media. https://doi.org/10.1007/978-1-4471-0785-9

[20] Utkin, V., Guldner, J., & Shi, J. (2017). *Sliding mode control in electro-mechanical systems*. CRC press. https://doi.org/10.1201/9781420065619

[21] Sánchez, E. N., & Djilali, L. (2020). *Neural Control of Renewable Electrical Power Systems* (Vol. 278). Springer Nature. https://doi.org/10.1007/978-3-030-47443-0

[22] Djilali, L., Sanchez, E. N., Ornelas-Tellez, F., Avalos, A., & Belkheiri, M. (2019). Improving microgrid low-voltage ride-through capacity using neural control. *IEEE Systems Journal*, *14*(2), 2825-2836. https://doi.org/10.1109/JSYST.2019.2947840

ISSN-2523-6830
ECORFAN® All rights reserved